


RESEARCH

Open Access



Multi-omics analysis of synovial tissue and fluid reveals differentially expressed proteins and metabolites in osteoarthritis

Minghao Ge^{1†}, Weihao Sun^{1,4†}, Tianhao Xu¹, Runze Yang¹, Kaibo Zhang¹, Jian Li¹, Zhiwei Zhao^{3*}, Meng Gong^{2*} and Weili Fu^{1*} 

Abstract

Background Knee osteoarthritis is a common degenerative joint disease involving multiple pathological processes, including energy metabolism, cartilage repair, and osteogenesis. To investigate the alterations in critical metabolic pathways and differential proteins in osteoarthritis patients through metabolomic and proteomic analyses and to explore the potential mechanisms underlying synovial osteogenesis during osteoarthritis progression.

Methods Metabolomics was used to analyze metabolites in the synovial fluid and synovium of osteoarthritis patients (osteoarthritis group: 10; control group: 10), whereas proteomics was used to examine differential protein expression. Alkaline phosphatase activity was assessed to evaluate osteogenesis.

Results Upregulation of the tricarboxylic acid cycle: Significant upregulation of the tricarboxylic acid cycle in the synovial fluid and synovium of osteoarthritis patients indicated increased energy metabolism and cartilage repair activity. Arginine metabolism and collagen degradation: Elevated levels of ornithine, proline, and hydroxyproline in the synovial fluid reflect active collagen degradation and metabolism, contributing to joint cartilage breakdown. Abnormal Phenylalanine Metabolism: Increased phenylalanine and tyrosine metabolite levels in osteoarthritis patients suggest their involvement in cartilage destruction and osteoarthritis progression. Synovial osteogenesis: Increased expression of type I collagen in the synovium and elevated alkaline phosphatase activity confirmed the occurrence of osteogenesis, potentially driven by the differentiation of synovial fibroblasts, mesenchymal stem cells, and hypertrophic chondrocytes. Relationships between differential proteins and osteogenesis: FN1 and TGFBI are closely associated with synovial osteogenesis, while the upregulation of energy metabolism pathways provides the energy source for osteogenic transformation.

[†]Minghao Ge and Weihao Sun contributed equally to this work.

*Correspondence:

Zhiwei Zhao

zzw2002400@126.com

Meng Gong

gongmeng@scu.edu.cn

Weili Fu

foxwin2008@163.com

Full list of author information is available at the end of the article



© The Author(s) 2025. **Open Access** This article is licensed under a Creative Commons Attribution-NonCommercial-NoDerivatives 4.0 International License, which permits any non-commercial use, sharing, distribution and reproduction in any medium or format, as long as you give appropriate credit to the original author(s) and the source, provide a link to the Creative Commons licence, and indicate if you modified the licensed material. You do not have permission under this licence to share adapted material derived from this article or parts of it. The images or other third party material in this article are included in the article's Creative Commons licence, unless indicated otherwise in a credit line to the material. If material is not included in the article's Creative Commons licence and your intended use is not permitted by statutory regulation or exceeds the permitted use, you will need to obtain permission directly from the copyright holder. To view a copy of this licence, visit <http://creativecommons.org/licenses/by-nc-nd/4.0/>.

Conclusions Alterations in energy metabolism, cartilage repair, and osteogenic mechanisms are critical. The related metabolites and proteins have potential as diagnostic and therapeutic targets for osteoarthritis.

Keywords Knee osteoarthritis, Proteomics, Metabolomics, Tricarboxylic acid cycle, Fibronectin 1

Background

Knee osteoarthritis (KOA) is the most common and damaging form of osteoarthritis, leading to significant societal and familial losses [1, 2]. With ongoing research, the definition of OA has evolved: it is characterized by a disruption in the balance of catabolism and anabolism of cartilage, subchondral bone, and the extracellular matrix (ECM) [3]. This disruption is influenced not only by mechanical factors but also by biological factors, which are critically important [4]. Initially, studies on the pathogenesis of KOA focused predominantly on mechanical factors, attributing its onset to age, mechanical wear, and trauma [1, 5]. Inflammation is thought to arise from a chronic load and compromised joint biomechanics, leading to symptoms such as joint swelling, stiffness, and limited mobility [6]. However, subsequent studies have revealed that the activation of immune responses, the release of free radicals, elevated intraosseous pressure, and the secretion of cytokines are integral to KOA pathogenesis, although the specific mechanisms involved remain fully understood [6]. Changes in subchondral bone in KOA patients are associated with mechanisms of elevated intraosseous pressure, which leads to necrosis of bone tissue and resorption and remodeling of necrotic trabecular bone, resulting in subchondral bone sclerosis. This, in turn, causes uneven stress on the cartilage, aggravating its deterioration [7]. Radiological examinations typically reveal vital features such as joint space narrowing, osteophyte formation, and subchondral bone necrosis, usually indicating advanced stages of KOA that have surpassed the optimal treatment window [4, 8]. Furthermore, the formation of free bodies in the knee often exacerbates pain and locking symptoms. Pathological changes occur well before clinical symptoms appear, with cartilage destruction central to the development of KOA, as increased destruction and reduced synthesis/repair of cartilage are the primary factors in its progression [9].

Throughout the progression of KOA, various changes in chondrocytes can be observed, characterized by the coexistence of necrosis and increased activity. The cartilage matrix also exhibited disordered collagen fiber arrangement and calcium crystal deposition. The pathology of subchondral bone primarily arises from microfractures, leading to trabecular necrosis. The formation of osteophytes is associated with subchondral bone repair mechanisms [10]. As the cartilage gradually degenerates, the smoothness of the articular surface decreases, exposing the bone ends. The body initiates bone repair

mechanisms in response to joint structure damage, leading to osteophyte formation at the joint margins [11, 12].

KOA is commonly accompanied by chronic inflammatory responses, with inflammatory cells from the synovium, cartilage, and surrounding tissues releasing various inflammatory mediators and growth factors, such as fibronectin 1 (FN1), transforming growth factor-beta (TGFBI), and fibroblast growth factor (FGF) [4, 13–15]. These factors stimulate the proliferation and differentiation of cells in the subchondral bone and synovium, promoting osteophyte formation. FN1 is a protein-coding gene associated with various diseases, including spondyloepiphyseal dysplasia, and its related pathways include signaling downstream of RAS mutations and integrin pathways. The gene ontology (GO) annotations related to this gene include heparin binding and protease binding. A significant paralog of this gene is TNC. TGF- β is a critical regulatory factor in osteophyte formation that plays a role in cartilage degeneration and stimulates the osteogenic differentiation of subchondral bone and synovial fibroblasts, promoting osteophyte development [16]. TGF- β may further exacerbate osteophyte growth by facilitating the differentiation of mesenchymal stem cells into osteoblasts [17].

Inflammatory cells from the synovium, cartilage, and surrounding tissues release various inflammatory mediators and growth factors, such as FN1. In recent years, single-omics technologies applied to multiple KOA samples (chondrocytes, synovial tissues, synovial fluid, plasma, and urine) have revealed numerous biomarkers associated with this disease; however, their mechanisms remain unclear [18]. It is well established that type I and type II collagen are the most abundant collagens in the bone and cartilage ECM, respectively [19]. Among the many KOA omics studies, the majority have focused on cartilage tissue, chondrocytes, plasma, and urine [20–22]. Moreover, research on the synovium and synovial fluid has been relatively limited, likely due to difficulties in obtaining samples. The synovium and synovial fluid may mediate inflammation and immune responses in KOA pathogenesis. Since synovial fluid is the sole source of the liquid microenvironment of the knee joint and the synovium is its secretion source, both are critical for comprehensively elucidating the pathogenesis of KOA. Therefore, this study aims to utilize human knee synovial tissue and synovial fluid samples, employing a combined approach of metabolomics and proteomics to identify differentially expressed biomarkers to provide theoretical insights into the mechanisms underlying the onset, progression, and

maintenance of KOA, as well as explore the potential mechanisms of osteogenesis in the synovium.

Methods

Ethical approval and patient inclusion

This project was approved by the Ethics Committee [Approval No. 2019(610)] and officially commenced in January 2018. All patients included in this study were part of this research sequence and signed informed consent forms preoperatively. The same medical team performed the preoperative diagnosis, surgical procedures, arthroscopic sample collection, and final diagnosis, with follow-up conducted by the authors. For this study, 10 patients with KOA were selected as the experimental group, and 10 healthy controls were included during the same period for the metabolomics and proteomics analyses. The baseline characteristics of the patients are provided in Table 1.

Inclusion criteria

KOA group: Patients were clinically diagnosed with knee osteoarthritis, with primary lesions in the medial or lateral compartments; aged 18–80 years; and received ineffective conservative treatment. Indications for synovectomy.

Control group: Patients with amputations (above the knee), extra-articular fractures, isolated meniscal injuries, or congenital discoid meniscus, with no synovial fluid or synovitis detected during arthroscopic exploration; age 18–80 years; and undergoing arthroscopic exploration, fracture fixation, joint replacement, or amputation.

All patients were initially assessed by physicians with 5–10 years of clinical experience through specialized interviews and physical examinations. Clinical characteristics were recorded, especially knee redness, swelling, warmth, pain severity, joint effusion, and deformities. Two radiologists with 5–10 years of experience independently evaluated X-rays and MR images. In the case of discrepancies, a senior radiologist made the final judgment. Arthroscopic exploration was performed to assess synovial tissue under direct visualization, as was cartilage damage and the presence of free bodies. Synovial tissue from multiple sites and synovial fluid were collected

during surgery. The samples were centrifuged, frozen in liquid nitrogen, and stored at -80 °C for subsequent analyses.

Data-Independent Acquisition (DIA) proteomics

Synovial tissue sample preparation: Synovial tissue was ground thoroughly after being removed from -80 °C storage. A mixture of 250 µL of PBS and protease inhibitors was added, followed by the addition of 250 µL of SDS lysis buffer for protein denaturation. The mixture was centrifuged at 8000 × g for 1 min, and the supernatant was collected. The sample was then heated and sonicated and centrifuged at 8000 × g for 15 min, after which a second supernatant was collected. The protein concentration was measured via a BCA kit.

Synovial fluid sample preparation: Synovial fluid samples were thawed and vortexed to remove high-abundance proteins.

Protein digestion and peptide quantification: Protein solutions were reduced and alkylated with dithiothreitol and iodoacetamide, followed by digestion with trypsin overnight at 37 °C via FASP filters (PALL, OD010C34). Peptides were quantified via a Thermo Fisher protein quantification kit (23275).

DIA Proteomics and LC-MS Analysis: Peptide samples were separated via low-pH reversed-phase C18 chromatography and analyzed on an Orbitrap Fusion Lumos mass spectrometer via DIA. The mass spectrometry parameters were set as follows: MSn level=1, Orbitrap resolution=60 K, scan range=350–1550 m/z, maximum injection time=50 ms, AGC target=1.0e6; MSn level=2, isolation window=1.6, collision energy=32%, Orbitrap resolution=30 K, AGC 5.0e5. Proteins were identified and quantified through database searches, and missing data were estimated via KNN algorithms. Proteins with >50% missing data or a coefficient of variation >30% were excluded. Differential proteins (*p*<0.05) were identified via ANOVA. Principal component analysis (PCA) and orthogonal partial least squares discriminant analysis (OPLS-DA) were subsequently conducted, followed by GO enrichment, KEGG pathway enrichment, and protein-protein interaction network analyses via STRING (<https://cn.string-db.org/>). Upstream regulators of synovial differential proteins were predicted via IPA software. Correlation networks were constructed on the basis of Pearson correlation coefficients (*r*>0.6 or *r*<-0.6) and visualized via Cytoscape.

Metabolomics

Synovial tissue sample preparation: Synovial tissue (10 mg per sample) was thawed at 4 °C, washed in PBS, and homogenized with 200 µL of precooled methanol-water (MeOH=4:1). After homogenization and ultra-sonication, the samples were centrifuged at 13,300 rpm

Table 1 Clinical characteristics of knee osteoarthritis patients with synovial hondromatosis vs. Normal subjects

	N	OA	P value
N	10	10	
Age, mean years (x±s)	52.4±12.0	55.9±10.8	0.502
male, n (10%)	1(10%)	3(30%)	0.264
BMI(X±s, kg/m ²)	24.3±2.8	25.6±3.3	0.369
Hospital length of stay, (X±s day)	4.1±0.7	4.7±0.8	0.103
ROM(X±s)	126.5±5.8	117.0±17.0	0
Lysholm (X±s, points)	67.8±5.7	53.1±7.2	0

for 30 min at 4 °C. The supernatants were pooled, dried, and resuspended in 200 µL of Hillic solution for further analysis.

Synovial fluid sample preparation: Synovial fluid samples were thawed and vortexed, followed by the addition of 250 µL of methanol. After centrifugation, the supernatant was resuspended in Hillic solution and prepared for analysis.

LC-MS/MS analysis: Samples were analyzed via a Thermo Q Exactive Plus mass spectrometer in positive and negative ion modes. Chromatographic separation was performed on an ACQUITY UPLC BEH amide column. Quality control samples (QCs) were prepared by pooling 20 µL of supernatant from each sample, and PCA was performed to assess the data quality.

Statistical analysis

Normality was tested via the Shapiro–Wilk test. Nonnormally distributed data were analyzed via the Wilcoxon rank-sum test, whereas customarily distributed data were analyzed via one-way ANOVA. A p value < 0.05 was considered statistically significant. Analyses were performed via IBM SPSS 22.0.

Results

Differential protein expression and functional enrichment analysis in the knee synovium

PCA was performed on the basis of protein expression data to visualize the relationships between the OA and N groups across different dimensions. Each point represents a replicate of the grouped experiments, with different colors distinguishing the groups (Supplementary Fig. 1A). The PCA demonstrated the precise spatial distribution within each group. In synovial proteomics, 174 differentially expressed proteins (DEPs) were identified, with 67 proteins upregulated and 107 downregulated (Supplementary Table 1, Supplementary Fig. 1B). A volcano plot further illustrated the significant differences in protein expression between the OA and control groups (Fig. 1A), and a heatmap confirmed the consistency of protein changes between the groups (Supplementary Fig. 2A). To explore the biological functions of the DEPs, GO enrichment analysis was performed, revealing associations with biological processes such as cell adhesion, extracellular matrix organization, and collagen fibril organization (Fig. 1B). These processes are closely linked to cartilage degradation and synovial chondromatosis formation in OA. KEGG pathway enrichment analysis revealed that the DEPs were significantly enriched in complement and coagulation cascades, ECM-receptor interactions, and focal adhesion pathways, all of which are related to cartilage degradation and matrix remodeling in synovial chondromatosis (Fig. 1C). Protein–protein interaction (PPI) analysis revealed significant associations

between FN1, TGFBI, COL1A1, COL3A1, and MMP2 (Fig. 1D), highlighting their roles in extracellular matrix organization and synovial cartilage formation in OA through the complement and coagulation cascades and focal adhesion pathways.

Proteomic analysis of synovial fluid

PCA of protein expression data from synovial fluid also revealed distinct spatial distributions between the OA and control groups (Supplementary Fig. 3A). In total, 15 DEPs were identified, with 8 upregulated and 7 downregulated (Supplementary Table 2, Supplementary Fig. 3B). The volcano plot revealed significant protein expression differences between the OA and control groups (Fig. 2A), and a heatmap confirmed the consistency of protein changes between the groups (Supplementary Fig. 4A). GO enrichment analysis of synovial fluid DEPs revealed associations with collagen matrix organization, extracellular matrix organization, and collagen binding, which are related to cartilage degradation and synovial chondromatosis formation in OA (Fig. 2B). KEGG pathway enrichment further revealed significant enrichment in the ECM-receptor interaction, complement and coagulation cascades, and focal adhesion pathways, similar to the results of the synovial proteomics analysis (Fig. 2C). PPI analysis revealed significant associations between FN1, TGFBI, COL1A1, and MMP3 (Fig. 2D), indicating that these proteins play essential roles in ECM remodeling and synovial cartilage formation in OA, with a trend similar to that observed in synovial tissue.

Integrated analysis and validation of synovial and synovial fluid differential proteins

KGML network analysis of both synovial and synovial fluid proteomics revealed that the proteins FN1, COL1A1, and COL3A1, which are significantly associated with the ECM-receptor interaction, focal adhesion, and complement and coagulation cascade pathways, were upregulated (Fig. 3A). ECM remodeling plays a critical role in the development of OA-associated synovial chondromatosis. Western blot analysis confirmed that the expression levels of FN1, COL1A1, COL3A1, and TGFBI were significantly greater in the OA group than in the control group (Fig. 3B, C). Immunohistochemistry further confirmed that FN1 and TGFBI expression in synovial tissue was significantly elevated in OA patients compared with the control group (Fig. 3D–F).

Metabolomic analysis of the synovium and synovial fluid of OA patients

Metabolomic profiling was subsequently performed to analyze the metabolic changes in the synovium and synovial fluid and investigate the underlying mechanisms of OA-associated synovial chondromatosis. QC sample

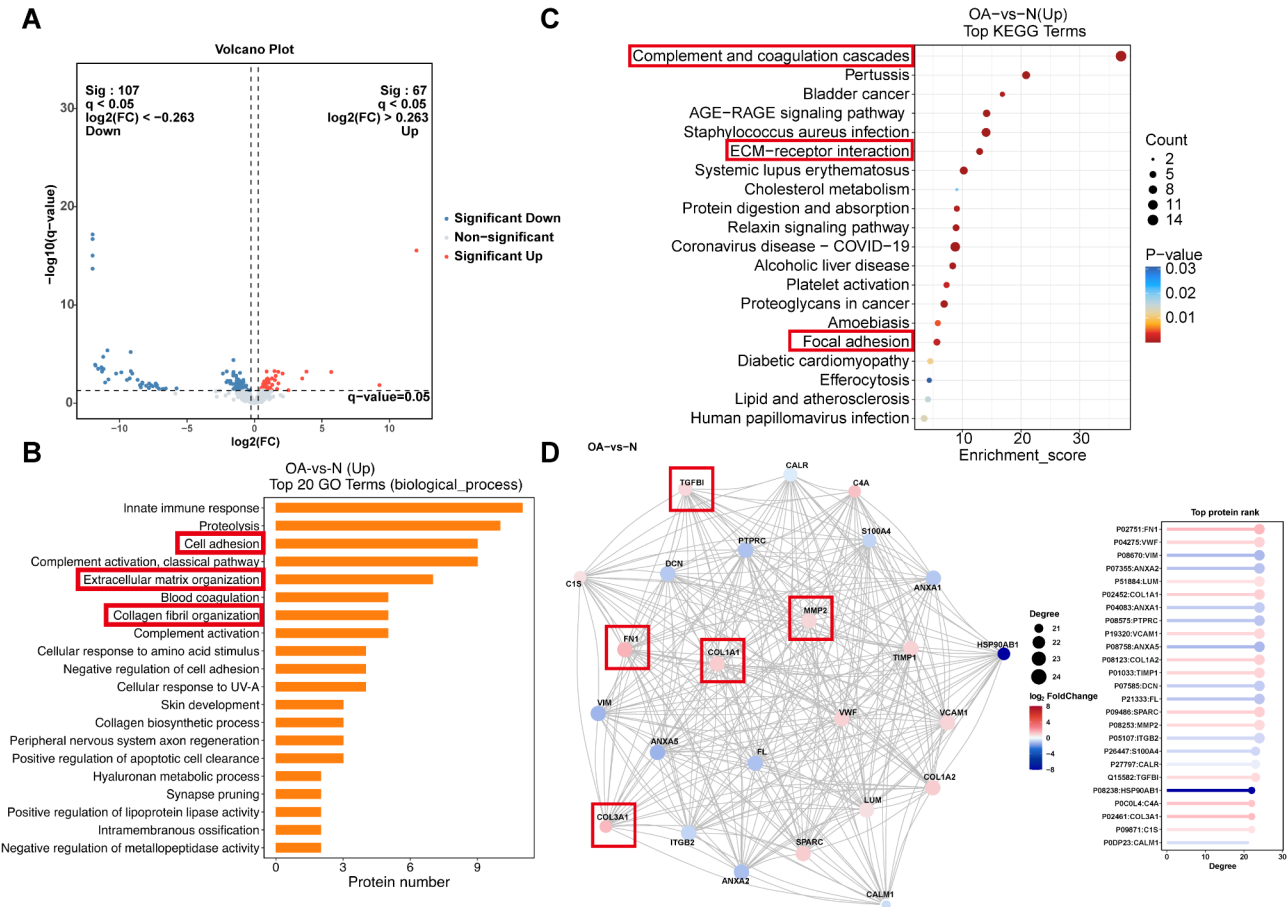


Fig. 1 Differential protein expression and functional enrichment analysis of the knee synovium. **(A)** Volcano plot of differentially expressed proteins in synovial tissue. The red dots represent proteins upregulated in the OA group compared with those in the N group, whereas the blue dots represent downregulated proteins. **(B)** GO enrichment analysis of differentially expressed proteins in synovial tissue, displaying the top 20 biological processes (List-Hits > 1, p value smallest). The x-axis shows the number of foreground proteins, and the y-axis lists the GO terms. **(C)** KEGG enrichment analysis of differentially expressed proteins in synovial tissue, showing the top 20 pathways. The x-axis represents the enrichment score, whereas the y-axis lists the pathways. **(D)** The left panel displays the protein–protein interaction network of the top 25 most connected differentially expressed proteins in synovial tissue, with red circles representing upregulated proteins, blue circles representing downregulated proteins, and the circle size indicating the degree of connectivity. The right panel shows a bar graph of protein expression for the top 25 most connected proteins. A shared legend is displayed between both panels

analysis confirmed the stability and reproducibility of the method (Supplementary Fig. 6A, 7A). Multivariate statistical analysis of the metabolomic data revealed clear group distinctions in the synovium (Supplementary Fig. 6B) and synovial fluid (Supplementary Fig. 7B). The OPLS-DA models demonstrated more distinct group separations, with R2Y and Q2 values both exceeding 0.5 (Fig. 4A, D). Four thousand four hundred eighty-four metabolites were identified in the synovium and 2,243 in synovial fluid, with 693 differentially abundant metabolites identified in the synovium and 341 in synovial fluid (Fig. 4B, E).

Among the differentially abundant metabolites, 328 were selected from the synovium (240 upregulated and 88 downregulated in OA), whereas 152 were chosen from synovial fluid (78 upregulated and 74 downregulated in OA). The two heatmaps confirmed the consistency of

metabolite differences between the synovial fluid and synovial fluid groups (Supplementary Fig. 6C and 7C). The list of differentially abundant metabolites in joint and synovial fluid is presented in Supplementary Tables 3 and Supplementary Table 4. KEGG pathway enrichment analysis significant enrichment of the TCA cycle and phenylalanine metabolism pathways in the synovium (Fig. 4C) and arginine biosynthesis and alanine, aspartate, and glutamate metabolism in synovial fluid (Fig. 4F). These pathways are linked to increased energy metabolism, promote bone and cartilage repair and contribute to osteophyte formation and irregular cartilage proliferation.

To validate these findings, we measured four metabolites in the synovium from both groups. Fumarate (TCA cycle), aspartate, arginine, and phenylalanine were significantly elevated in OA patients (Fig. 5A, B and C, D), confirming the increased expression of key metabolites

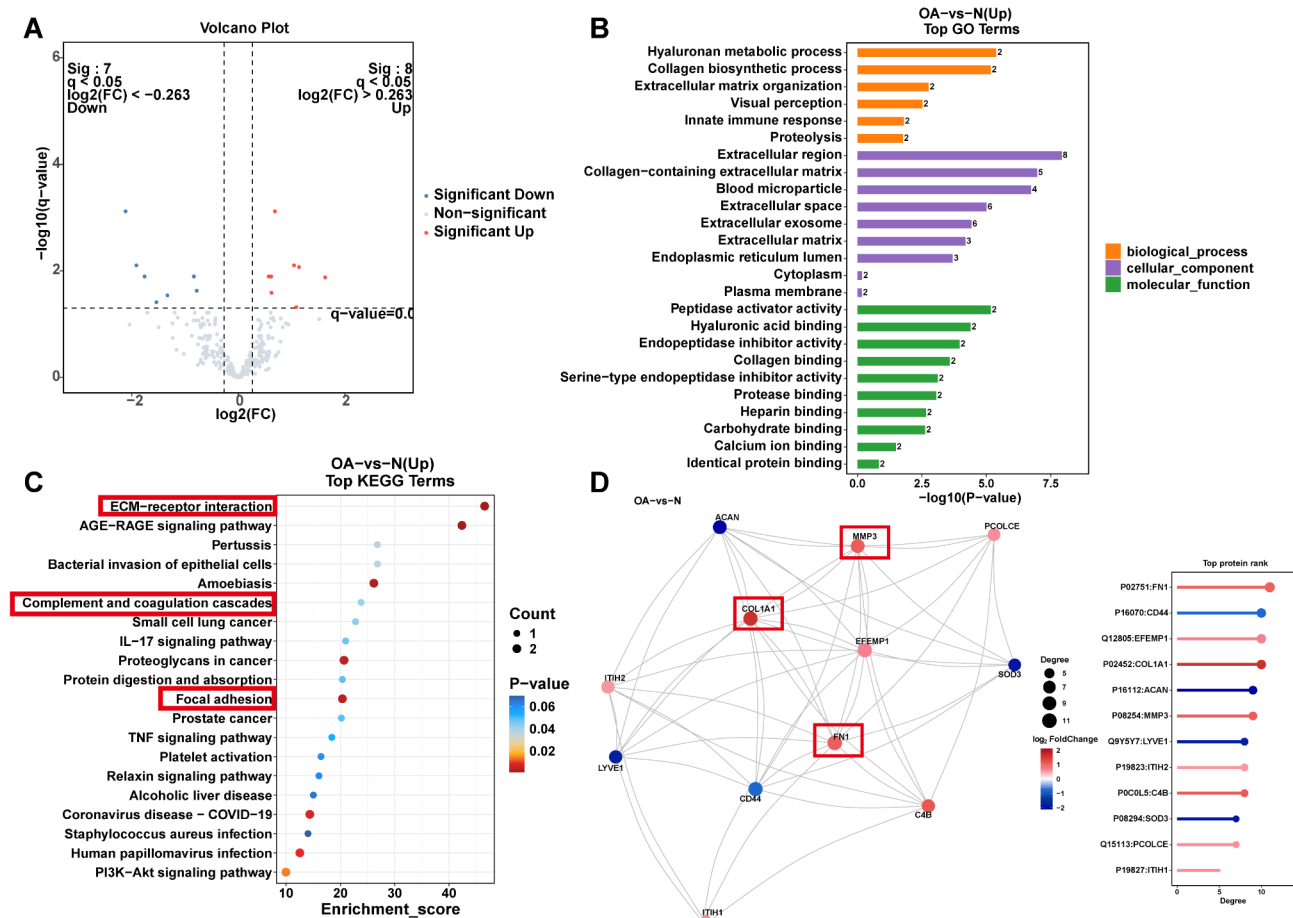


Fig. 2 Proteomic analysis of synovial fluid. **(A)** Volcano plot of differentially expressed proteins in synovial fluid. The red dots represent proteins upregulated in the OA group, whereas the blue dots represent downregulated proteins. **(B)** GO enrichment analysis of differentially expressed proteins in synovial fluid, showing the top 30 biological processes (selected from the three ontologies with ListHits > 1, p value smallest). The x-axis shows the number of foreground proteins, and the y-axis lists the GO terms. **(C)** KEGG enrichment analysis of differentially expressed proteins in synovial fluid, showing the top 20 pathways. The x-axis represents the enrichment score, whereas the y-axis lists the pathways. **(D)** The left panel displays the protein-protein interaction network of the top 25 most connected differentially expressed proteins in synovial fluid, with red circles representing upregulated proteins, blue circles representing downregulated proteins, and the circle size indicating the degree of connectivity. The right panel shows a bar graph of protein expression for the top 25 most connected proteins. A shared legend is displayed between both panels

in the TCA cycle and energy metabolism pathways. The results revealed a significant increase in ALP activity in KOA patients (Supplementary Fig. 5A).

Integrated proteomic and metabolomic analysis in OA patients

We conducted combined proteomic and metabolomic analyses of OA patients on the basis of differentially abundant metabolite and protein screening results, KEGG pathway enrichment, functional analysis, IPA upstream regulator analysis, and protein-protein interaction (PPI) network analysis. Boxplots revealed significant differences in the expression of differentially expressed proteins between the two groups (Fig. 6A, C). The findings revealed that VWF, FN1, and TGFBI promote synovial chondromatosis through ECM remodeling and the COL1A1 and COL3A1 signaling pathways (Fig. 6B).

Furthermore, critical metabolites from alanine, aspartate, and glutamate metabolism; arginine biosynthesis; and phenylalanine metabolism (e.g., aspartic acid, L-glutamate, ornithine, phenylalanine) collectively increased fumaric acid levels, thereby enhancing the TCA cycle (Fig. 1). 6B, D, E). This metabolic reprogramming provides substantial energy for ECM remodeling and synovial osteogenesis, as illustrated in Fig. 6B.

Discussion

Under normal physiological conditions, chondrocytes regulate cartilage metabolism, maintaining a balance between anabolic and catabolic processes to ensure cartilage homeostasis [23]. Throughout the progression of KOA, chondrocytes are influenced by various factors. First, biomechanical stimuli, such as increased stress from obesity, compression from intra-articular

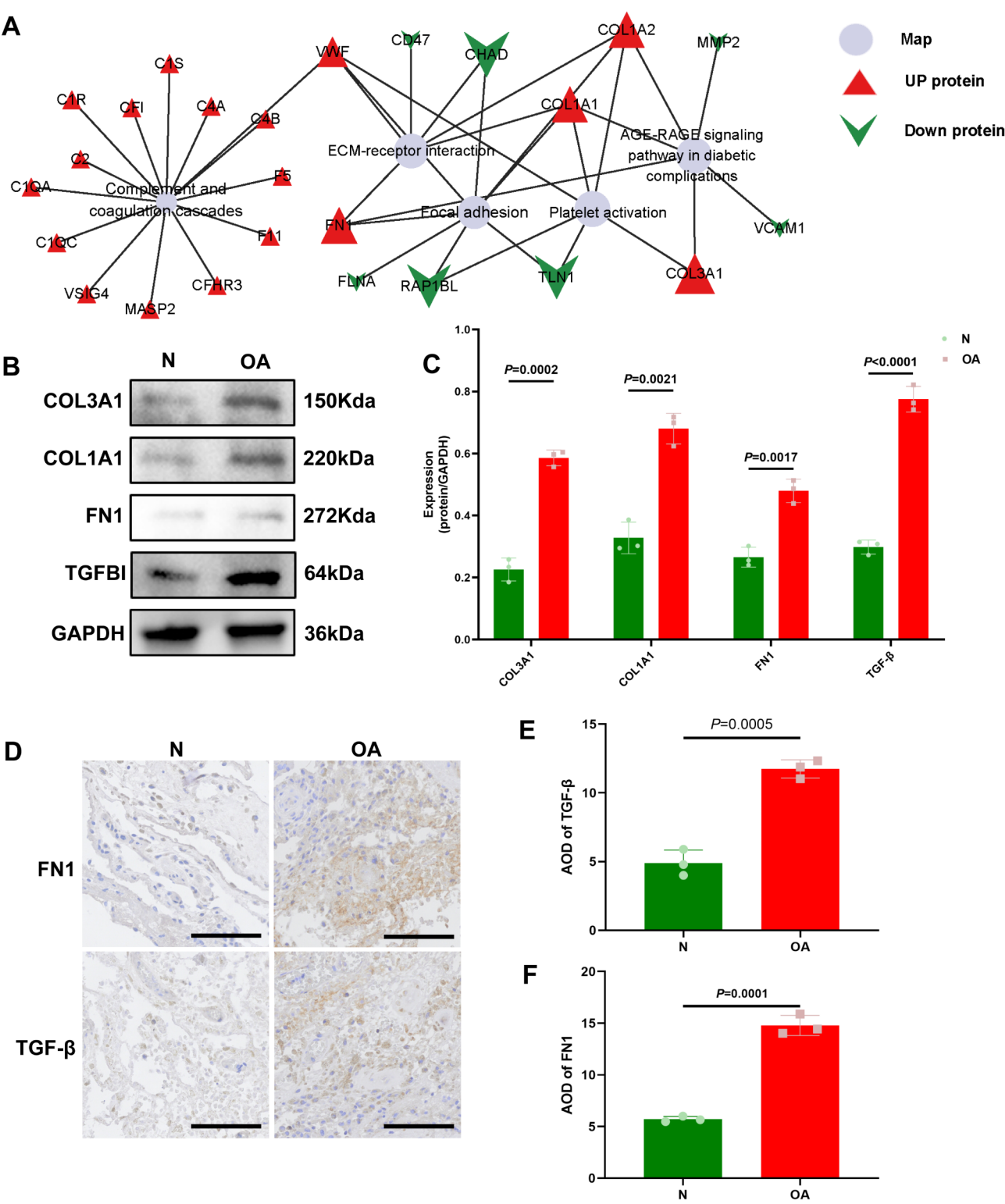


Fig. 3 Integrated analysis and validation of Synovial and Synovial Fluid Differential proteins. **(A)** Example of the KGML network showing the relationships between differentially expressed proteins in synovial tissue and synovial fluid. Red triangles represent upregulated proteins, and green arrows represent downregulated proteins. **(B)** The expression levels of COL3A1, COL1A1, FN1, and TGFBI were evaluated via western blotting. **(C)** Quantification of COL3A1, COL1A1, FN1, and TGFBI expression ($n = 3$; data are expressed as the means \pm SDs; two-way ANOVA followed by Tukey's post hoc test). * indicates $P < 0.05$, ** indicates $P < 0.01$, *** indicates $P < 0.001$. **(D)** IHC staining of FN1 and TGFBI in OA and normal (N) samples (scale bar = 100 μ m). **(E, F)** Quantitative analysis of FN1 and TGFBI immunohistochemistry results ($n = 3$; the data are expressed as the means \pm SDs; two-way ANOVA followed by Tukey's post hoc test)

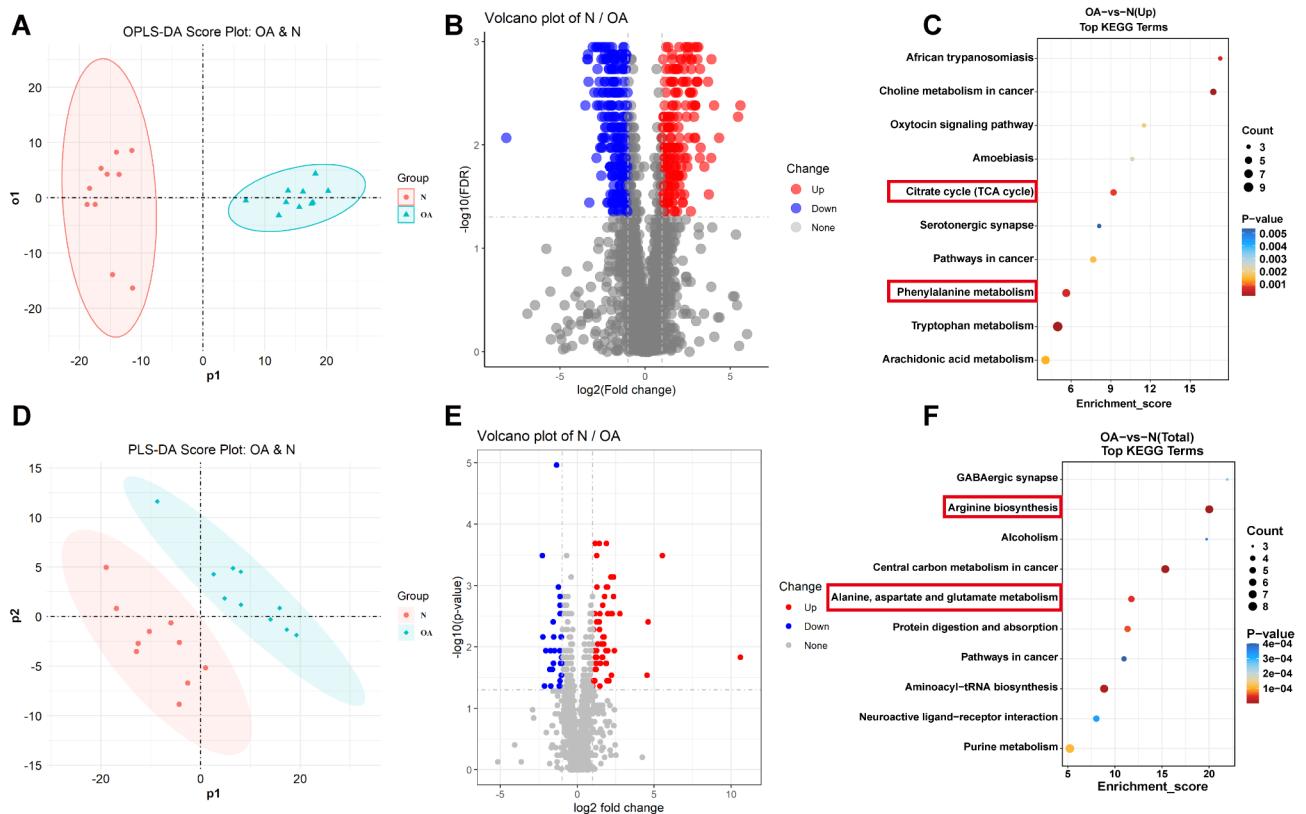


Fig. 4 Metabolomic analysis of the synovium and synovial fluid of OA patients. **(A)** OPLS-DA plot of the metabolomic data from the synovial samples of both groups. **(B)** Volcano plot of differentially expressed metabolites in synovial tissue. The red dots represent significantly upregulated metabolites in the OA group, the blue dots represent significantly downregulated metabolites, and the gray dots represent nonsignificant metabolites. **(C)** Bubble plot of the pathway enrichment analysis of the upregulated metabolites in synovial tissue showing the top 10 pathways. The x-axis represents the enrichment score, and the y-axis represents the pathways. The larger the bubble is, the greater the number of metabolites involved, and the color transition from blue to red indicates greater significance (smaller p value). **(D)** OPLS-DA plot of the metabolomic data from the synovial fluid samples of both groups. **(E)** Volcano plot of differentially expressed metabolites in synovial fluid. The red dots represent significantly upregulated metabolites in the OA group, the blue dots represent significantly downregulated metabolites, and the gray dots represent nonsignificant metabolites. **(F)** Bubble plot of pathway enrichment analysis of differentially expressed metabolites in synovial fluid showing the top 10 pathways. The x-axis represents the enrichment score, and the y-axis represents the pathways. The larger the bubble is, the greater the number of metabolites involved, and the color transition from blue to red indicates greater significance (smaller p value).

loose bodies, and uneven joint loading due to cartilage degeneration, disrupt the balance between cartilage synthesis and degradation, exacerbating cartilage damage. Mechanical loading activates mechanoreceptors, including mechanosensitive ion channels and integrins, on the surface of chondrocytes [24]. Additionally, the onset of inflammation plays a critical role in cartilage degradation. The formation of cartilage degradation products, including damage-associated molecular patterns (DAMPs), leads to the release of proinflammatory cytokines. Once released into the joint cavity, these cytokines stimulate synovial hyperplasia and perpetuate inflammation, contributing to synovitis and accelerating cartilage breakdown [25]. The synovium, which is composed of intimal and subintimal layers, is typically approximately 5 mm thick in a healthy joint [26]. Previous KOA studies have identified two types of macrophages within the

synovium: classical macrophages and inflammatory macrophages [27].

Synovial fluid, which is secreted by the synovium, plays a critical role in cartilage nutrition and consists of synovium-derived hyaluronan–protein complexes and plasma-derived exudates. As the fluid is in direct contact with articular cartilage, synovial fluid is the primary regulator of the joint's physiological microenvironment. Owing to the avascular nature of cartilage, synovial fluid is the main source of nutrients and the primary reservoir for cartilage degradation products [28, 29].

In this study, we utilized DIA proteomics to analyze the protein profiles of synovium and synovial fluid from KOA patients. We identified 90 significantly altered proteins with biological functions in the synovium, including 41 upregulated and 49 downregulated proteins. One hundred fifty-five differentially expressed proteins were identified in the synovial fluid, with 8 upregulated and

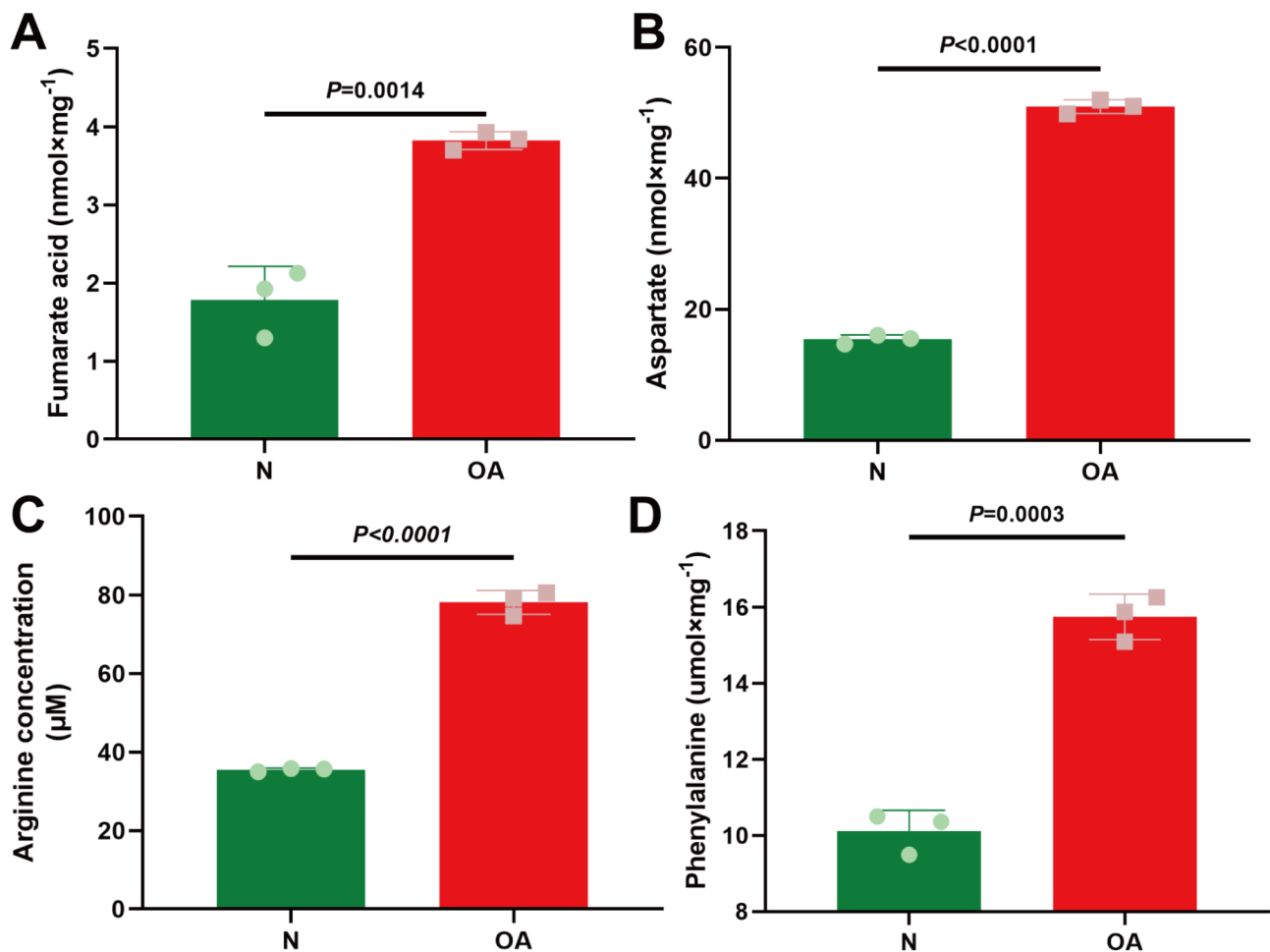


Fig. 5 Integrated proteomic and metabolomic analysis in OA patients. **(A)** Fumarate levels in synovial tissue from OA patients (OA group) versus the normal group (N group), $P=0.0014$. **(B)** Levels of aspartate in synovial tissue from KOA patients versus the normal group, $P<0.0001$. **(C)** Arginine levels in the synovial tissue of OA patients compared with those in the normal controls, $P<0.0001$. **(D)** Phenylalanine levels in the synovial tissue of KOA patients compared with those in the normal controls, $P=0.0003$

7 downregulated. GO enrichment analysis revealed that the differentially expressed proteins in both the synovium and synovial fluid were involved in cell adhesion, extracellular matrix organization, and collagen fibril organization, suggesting a shared biological function between these tissues in KOA pathology. KEGG pathway analysis revealed significant enrichment in the complement and coagulation cascades, ECM-receptor interaction, and focal adhesion pathways in the synovium, with all pathways showing upregulation. Interestingly, the ECM-receptor interaction pathway was inhibited in both the synovium and synovial fluid, indicating persistent ECM activity.

FN1 was significantly upregulated in both the synovium and synovial fluid. Previous studies have shown that FN1 contributes to cartilage fibrosis in OA by affecting collagen deposition, particularly by activating type III collagen. Transforming TGFBI is crucial for initiating immune cell differentiation and has been shown to induce

antiangiogenic effects during critical stages of angiogenesis by inhibiting MMP-2 [29, 30]. Increased CD4+ T-cell subsets, high concentrations of TGFBI, and angiogenesis are associated with the pathogenesis of OA, with TGF- β -dependent Smad2/3 phosphorylation and angiogenesis delaying cartilage degeneration and subchondral bone sclerosis, contributing to the progression of OA-related synovial chondromatosis [31].

ECM degradation is regulated primarily by MMPs, which are secreted by chondrocytes and synovial cells. MMP3 is typically secreted by chondrocytes and plays a crucial role in degrading the ECM and basement membranes [32, 33]. In our study, MMP3 and MMP2 were upregulated in the synovium and synovial fluid of KOA patients. Additionally, TIMP1 was upregulated in the synovium of KOA patients. MMPs and their corresponding TIMPs are usually cosecreted by the same cells. When both are highly expressed, MMP3 levels are twice as high as TIMP1 levels, suggesting an active ECM

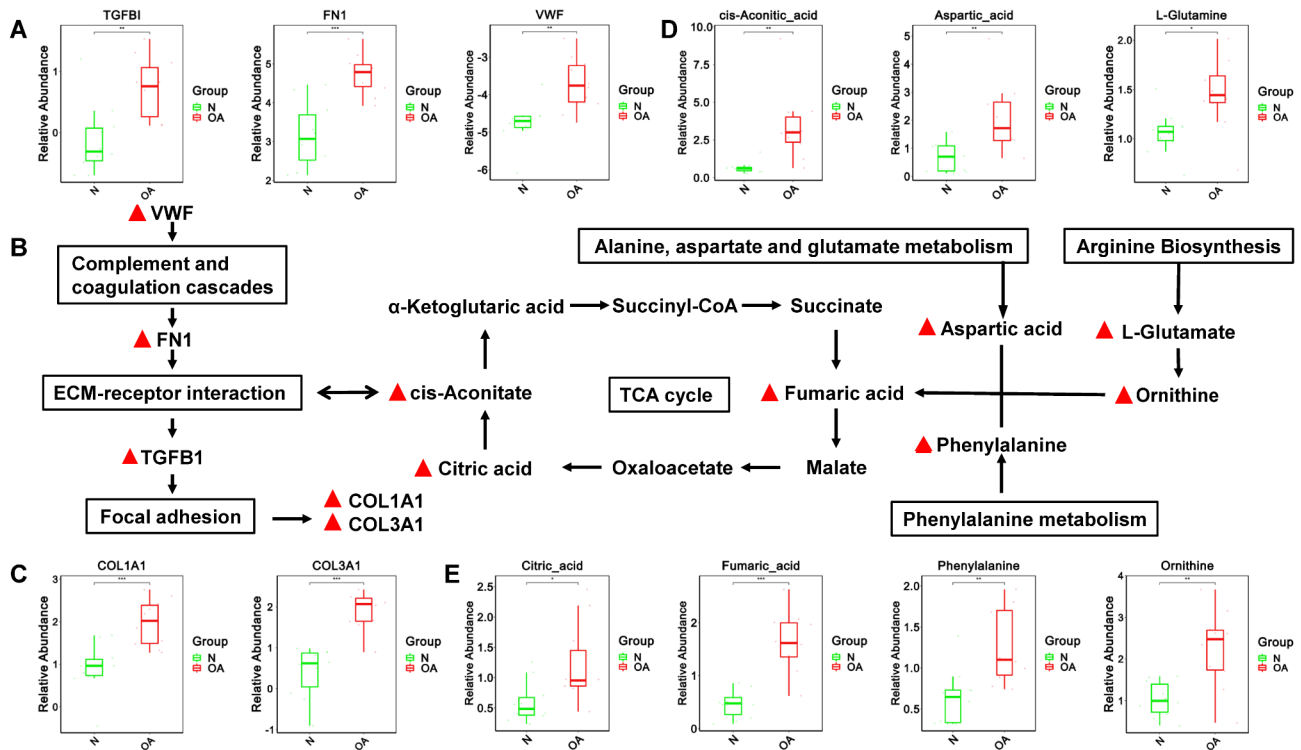


Fig. 6 Integrated proteomic and metabolomic analysis in OA patients. (A, C, D, E) Box plots showing the relative abundance of proteins and metabolites between the OA and control groups. The green boxes represent the control group, and the red boxes represent the OA group. * indicates $P < 0.05$, ** indicates $P < 0.01$, *** indicates $P < 0.001$, **** indicates $P < 0.0001$. (B) Metabolic network of significantly differentially expressed metabolites and proteins in synovial tissue and fluid, with red triangles indicating upregulated expression in the OA group

degradation process in the KOA synovium, with disruption of the TIMP1/MMP3 regulatory balance, contributing to KOA pathology.

In the normal synovium, collagen is almost absent; however, in our study, COL1A1 was highly expressed in the synovium and synovial fluid of KOA patients. Previous studies on KOA cartilage have reported a decrease in COL2A1 and an increase in COL1A1 during KOA progression, likely due to a shift from type II to type I collagen and the formation of osteophytes. Nonetheless, no studies have identified this phenomenon in the synovium or synovial fluid. Our findings suggest that synovial osteogenesis may occur at advanced KOA stages, as indicated by the formation of loose bodies with osteogenic characteristics that are detectable via radiological imaging (X-ray, MRI). Further research is needed to elucidate the specific mechanisms involved in this process.

We also performed metabolomics analysis via LC-MS/MS and identified 328 significantly altered water-soluble metabolites in the synovium of KOA patients, including 240 upregulated and 88 downregulated metabolites. These metabolites were enriched in pathways such as riboflavin metabolism, phenylalanine metabolism and biosynthesis, the TCA cycle, and linoleic acid metabolism. In the synovial fluid, 152 metabolites were significantly altered, with 78 upregulated and 74

downregulated, and pathways such as arginine biosynthesis, linoleic acid metabolism, alanine, aspartate, and glutamate metabolism, purine metabolism, and the TCA cycle were enriched.

Previous metabolomic analyses of synovial tissue in KOA have shown elevated levels of several TCA cycle intermediates, including citrate, aconitate, and malate, indicating the upregulation of this pathway in KOA. This finding is highly consistent with our study. Additionally, we observed significant increases in the TCA cycle intermediates succinate and glutamine, which can be derived from α -ketoglutarate. Research on synovial fluid indicates that KOA patients exhibit higher metabolite levels in the TCA cycle and glycolysis than those with rheumatoid arthritis. Elevated TCA cycle activity in the synovium and synovial fluid reflects a high-energy metabolic state.

Arginine is a semiessential amino acid that serves as a precursor for various molecules, including urea, nitric oxide, proline, glutamate, creatine, and agmatine. Ornithine can form a metabolic precursor for proline, a critical amino acid enriched in collagen, aiding in synthesizing collagen and polyamines and promoting cellular proliferation linked to fibrosis [34]. Our study revealed significantly elevated levels of ornithine, proline, and hydroxyproline in the synovial fluid of KOA patients compared with those of controls, with pathway analysis

revealing significant enrichment in the arginine biosynthesis pathway. Hydroxyproline, which is primarily found in collagen, is virtually absent from other proteins; its elevation reflects increased collagen degradation activity. Notably, no differences in ornithine, proline, or hydroxyproline levels were observed in the synovium, further suggesting that the high levels of hydroxyproline in synovial fluid originate from joint degradation, leading to the release of significant amounts of hydroxyproline from the breakdown of type II collagen. Therefore, the increased levels of these amino acids in synovial fluid indicate that cartilage degradation surpasses synthesis, contributing to the progression of KOA and suggesting potential as diagnostic biomarkers.

Research has indicated that elevated phenylalanine levels are associated with osteophyte formation in KOA [34]. Given this context, we speculate that high levels of phenylalanine may exacerbate cartilage damage by promoting the deposition of homogentisic acid in joint cartilage, leading to KOA progression. Our study revealed increased levels of phenylalanine in the synovium of KOA patients, along with elevated levels of tyrosine, a metabolite of phenylalanine, with KEGG analysis revealing upregulation of both phenylalanine metabolism and synthesis pathways. This finding indicates a high metabolic state in both the synthesis and degradation of phenylalanine, suggesting its close association with KOA progression.

Through metabolomics and proteomics, our study revealed the expression of COL1A1 in the synovium of KOA patients. To investigate whether osteogenesis occurred in the synovium, we assessed the activity of alkaline phosphatase (ALP), a critical marker of osteogenesis. The results revealed a significant increase in ALP activity in KOA patients, suggesting that the primary reason for the high expression of COL1A1 is the occurrence of synovial osteogenesis. One limitation of this study is the relatively small sample size, particularly in the validation cohort for synovial tissue and synovial fluid analyses. This limitation stems primarily from the challenges associated with obtaining these specialized samples from patients with osteoarthritis (OA), as they require invasive procedures such as arthrocentesis or joint replacement surgery and are not routinely collected in clinical practice. Owing to the small sample size, we were unable to perform certain analyses, such as correlating omics findings with clinical severity indices (e.g., Kellgren-Lawrence grade, WOMAC scores, or VAS for pain), which could provide further insights into the translational potential of the identified biomarkers in OA progression and severity [35]. Despite these constraints, we carefully selected samples that were representative of the OA disease spectrum, including patients at different stages of joint degeneration, and employed rigorous statistical

methods to minimize the impact of potential randomness and enhance the reliability of our results.

To address these limitations, future studies should aim to expand the cohort size and include additional clinical data, such as radiographic assessments (e.g., Kellgren-Lawrence grading), functional disability scores (e.g., WOMAC), and patient-reported outcomes (e.g., VAS for pain) [36]. Collaborative efforts with multiple clinical centers, particularly those specializing in orthopedic surgery and rheumatology, may also help overcome the challenges of sample collection and facilitate larger-scale validation studies [37]. By doing so, we hope to further strengthen the generalizability of our findings and validate the identified biomarkers as potential diagnostic or prognostic tools for OA.

First, fibroblasts possess inherent osteogenic capacity [12]. Synovial fibroblasts are widely present in the connective tissues surrounding joints and originate from synovial mesenchymal stem cells. The fibrotic scar tissue formed during repair can undergo calcification, leading to bone formation [38]. Numerous *in vitro* experiments on ligament fibroblasts have demonstrated that growth factors such as BMP, TGFBI, and IGF-1 can induce osteogenic or chondrogenic differentiation. Similarly, synovial fibroblasts possess differentiation capabilities *in vivo*, although such differentiation is typically quiescent under normal conditions [39]. However, numerous *in vivo* studies have indicated that fibroblasts can transform into osteoblasts under specific stimuli. These studies suggest that synovial fibroblasts possess substantial osteogenic potential, although the mechanisms underlying this differentiation in the absence of exogenous stimulation remain unclear. We hypothesize that the progression of KOA may induce the transformation of synovial fibroblasts into osteoblasts due to an inflammatory microenvironment or free bone fragments. In addition to the capacity of synovial fibroblasts to differentiate under certain conditions, synovial mesenchymal stem cells also exhibit osteogenic differentiation potential. Research has indicated that exogenous COL1 can promote the osteogenic conversion of mouse synovial mesenchymal stem cells and contribute to matrix mineralization [40]. Our findings suggest that as type I collagen increases during the progression of KOA, it may further induce the differentiation of synovial mesenchymal stem cells into osteoblasts. Moreover, chondrocytes undergo a process of proliferation and terminal hypertrophy, with hypertrophic chondrocytes confirmed to possess multidirectional differentiation potential, including the ability to promote osteoblast formation directly. During KOA progression, cartilage degradation can lead to the shedding of cartilage chunks, which, along with synovial fluid, may eventually be encapsulated by the proliferating synovium. Therefore, there is a possibility that chondrocytes are

present in the synovium of KOA patients, indicating the potential for hypertrophic chondrocytes to differentiate into osteoblasts. The differential proteins FN1 and TGFBI identified in our proteomic analysis are closely associated with synovial osteogenesis. In contrast, metabolomic analysis revealed that high energy metabolism (TCA cycle) expression provides the energy required for synovial osteogenic transformation.

Conclusions

Alterations in energy metabolism, cartilage repair, and osteogenic mechanisms are critical. The related metabolites and proteins have potential as diagnostic and therapeutic targets for osteoarthritis.

Abbreviations

ALP	Alkaline phosphatase
ANOVA	Analysis of variance
BCA	Bicinchoninic acid
DEPs	Differentially expressed proteins
DAMPs	Damage-associated molecular patterns
DIA	Data-independent acquisition
ECM	Extracellular matrix
KEGG	Kyoto Encyclopedia of Genes and Genomes
GO	Gene ontology
KOA	Knee osteoarthritis
KNN	k-nearest neighbor
LC-MS	Liquid chromatography–mass spectrometry
MRI	Magnetic resonance imaging
OPLS-DA	Orthogonal partial least squares discriminant analysis
PBS	Phosphate-buffered saline
QCs	Quality control samples
PPI	Protein–protein interaction
TCA cycle	Tricarboxylic acid cycle

Supplementary Information

The online version contains supplementary material available at <https://doi.org/10.1186/s12967-025-06310-y>.

Supplementary Material 1

Supplementary Material 2

Supplementary Material 3

Supplementary Material 4

Supplementary Material 5

Acknowledgements

Thank Yi Zhong, Tao Su, and Shisheng Wang (West China Hospital, Sichuan University) for relative data acquisition and analysis.

Author contributions

MG: Data curation, Formal analysis, Validation, Visualization, Writing – original draft; WS: Data curation, Formal analysis, Methodology, Writing – original draft; TX: Data curation, Methodology; RY: Project administration, Validation; KZ: Changes to the content during the revision process, as well as adjustments to the images; JL: Conceptualization, Funding acquisition, Methodology, Project administration; ZZ: Guidance on content writing during the revision process and review of the thesis – review & editing; MG: Conceptualization, project administration, resources, supervision, writing – review & editing; WF: Conceptualization, Funding acquisition, Project administration, Supervision, Writing – review & editing.

Funding

This study was funded by the National Natural Science Foundation of China (82172508, 82372490); the Sichuan Science and Technology Program (2024NSFJQ0041); the 1.3.5 Project for Disciplines of Excellence of West China Hospital Sichuan University (ZYJC21030).

Data availability

The datasets generated and/or analyzed during the current study are not publicly available because of ongoing patent applications related to the data. However, they are available from the corresponding author upon reasonable request.

Declarations

Ethics approval and consent to participate

This project was approved by the Ethics Committee [Approval No. 2019(610)] and officially commenced in January 2018. All patients included in this study were part of this research sequence and signed informed consent forms preoperatively.

Consent for publication

All the authors have read and approved the final version of the manuscript for submission.

Conflict of interest

The authors have no conflicts of interest.

Author details

¹Sports Medicine Center, Department of Orthopedic Surgery, Orthopedic Research Institute, West China Hospital, Sichuan University, Chengdu, Sichuan 610041, China

²Laboratory of Clinical Proteomics and Metabolomics, Institutes for Systems Genetics, Frontiers Science Center for Disease-related Molecular Network, National Clinical Research Center for Geriatrics, West China Hospital, Sichuan University, Chengdu, Sichuan 610041, China

³West China School of Basic Medical Sciences and Forensic Medicine, Sichuan University, Chengdu, Sichuan 610041, China

⁴Beijing Jishuitan Hospital, Capital Medical, 31 Dongjiekou East Street, Xicheng District, Beijing 110000, China

Received: 14 January 2025 / Accepted: 23 February 2025

Published online: 06 March 2025

References

- Glyn-Jones S, Palmer AJR, Agricola R, Price AJ, Vincent TL, Weinans H, et al. Osteoarthritis Lancet. 2015;386:376–87.
- Hodgkinson T, Kelly DC, Curtin CM, O'Brien FJ. Mechanosignalling in cartilage: an emerging target for the treatment of osteoarthritis. Nat Rev Rheumatol. 2022;18:67–84.
- Gong Z, Wang K, Chen J, Zhu J, Feng Z, Song C, et al. CircZSWIM6 mediates dysregulation of ECM and energy homeostasis in ageing chondrocytes through RPS14 post-translational modification. Clin Transl Med. 2023;13:e1158.
- Yao Q, Wu X, Tao C, Gong W, Chen M, Qu M, et al. Osteoarthritis: pathogenic signaling pathways and therapeutic targets. Signal Transduct Target Ther. 2023;8:56.
- Gelber AC. Knee osteoarthritis. Ann Intern Med. 2024;177:ITC129–44.
- Sanchez-Lopez E, Coras R, Torres A, Lane NE, Guma M. Synovial inflammation in osteoarthritis progression. Nat Rev Rheumatol. 2022;18:258–75.
- Hu W, Chen Y, Dou C, Dong S. Microenvironment in subchondral bone: predominant regulator for the treatment of osteoarthritis. Ann Rheum Dis. 2020;80:413.
- Zhan M, Sun H, Wang Z, Li G, Yang R, Mignani S, et al. Nanoparticle-Mediated multiple modulation of bone microenvironment to tackle osteoarthritis. ACS Nano. 2024;18:10625–41.
- Sun K, Guo J, Guo Z, Hou L, Liu H, Hou Y, et al. The roles of the Hippo-YAP signalling pathway in cartilage and osteoarthritis. Ageing Res Rev. 2023;90:102015.

10. Rf S, de Mh W, A L et al. S, T.V., Alarmins S100A8/S100A9 aggravate osteophyte formation in experimental osteoarthritis and predict osteophyte progression in early human symptomatic osteoarthritis. *Annals of the rheumatic diseases* [Internet]. 2016 [cited 2024 Oct 23];75. Available from: <https://pubmed.ncbi.nlm.nih.gov/25180294/>
11. Brylka LJ, Alimy A-R, Tschaffon-Müller MEA, Jiang S, Ballhause TM, Baranowsky A, et al. Piezo1 expression in chondrocytes controls endochondral ossification and osteoarthritis development. *Bone Res.* 2024;12:12.
12. Roelofs AJ, Kania K, Rafipay AJ, Sambale M, Kuwahara ST, Collins FL, et al. Identification of the skeletal progenitor cells forming osteophytes in osteoarthritis. *Ann Rheum Dis.* 2020;79:1625–34.
13. Liu B, Xian Y, Chen X, Shi Y, Dong J, Yang L, et al. Inflammatory Fibroblast-Like Synoviocyte-Derived exosomes aggravate osteoarthritis via enhancing macrophage Glycolysis. *Adv Sci (Weinh).* 2024;11:e2307338.
14. Liu Q, Han M, Wu Z, Fu W, Ji J, Liang Q, et al. DDX5 inhibits hyaline cartilage fibrosis and degradation in osteoarthritis via alternative splicing and G-quadruplex unwinding. *Nat Aging.* 2024;4:664–80.
15. Li H-Z, Zhang J-L, Yuan D-L, Xie W-Q, Ladel CH, Mobasher A, et al. Role of signaling pathways in age-related orthopedic diseases: focus on the fibroblast growth factor family. *Mil Med Res.* 2024;11:40.
16. van der Kraan PM. The changing role of TGFβ in healthy, ageing and Osteoarthritic joints. *Nat Rev Rheumatol.* 2017;13:155–63.
17. Zhen G, Wen C, Jia X, Li Y, Crane JL, Mears SC, et al. Inhibition of TGF-β signaling in mesenchymal stem cells of subchondral bone attenuates osteoarthritis. *Nat Med.* 2013;19:704–12.
18. Fan Y, Bian X, Meng X, Li L, Fu L, Zhang Y, et al. Unveiling inflammatory and prehypertrophic cell populations as key contributors to knee cartilage degeneration in osteoarthritis using multi-omics data integration. *Ann Rheum Dis.* 2024;83:926–44.
19. Johnston SA. Osteoarthritis. Joint anatomy, physiology, and pathobiology. *Vet Clin North Am Small Anim Pract.* 1997;27:699–723.
20. Nielsen RL, Monfeuga T, Kitchen RR, Egerod L, Leal LG, Schreyer ATH, et al. Data-driven identification of predictive risk biomarkers for subgroups of osteoarthritis using interpretable machine learning. *Nat Commun.* 2024;15:2817.
21. Fan Y, Bian X, Meng X, Li L, Fu L, Zhang Y, et al. Unveiling inflammatory and prehypertrophic cell populations as key contributors to knee cartilage degeneration in osteoarthritis using multi-omics data integration. *Ann Rheum Dis.* 2024;83:926.
22. Kreitmaier P, Katsoula G, Zeggini E. Insights from multi-omics integration in complex disease primary tissues. *Trends Genet.* 2023;39:46–58.
23. Rahman MM, Watton PN, Neu CP, Pierce DM. A chemo-mechano-biological modeling framework for cartilage evolving in health, disease, injury, and treatment. *Comput Methods Programs Biomed.* 2023;231:107419.
24. Jørgensen AEM, Kjær M, Heinemeier KM. The effect of aging and mechanical loading on the metabolism of articular cartilage. *J Rheumatol.* 2017;44:410–7.
25. Barnett R. Osteoarthritis. *Lancet.* 2018;391:1985.
26. Griffin TM, Scanzello CR. Innate inflammation and synovial macrophages in osteoarthritis pathophysiology. *Clin Exp Rheumatol.* 2019;37(Suppl 120):57–63.
27. Xie J, Huang Z, Yu X, Zhou L, Pei F. Clinical implications of macrophage dysfunction in the development of osteoarthritis of the knee. *Cytokine Growth Factor Rev.* 2019;46:36–44.
28. Schmidt TA, Gastelum NS, Nguyen QT, Schumacher BL, Sah RL. Boundary lubrication of articular cartilage: role of synovial fluid constituents. *Arthritis Rheum.* 2007;56:882–91.
29. Matheson AR, Sheehy EJ, Jay GD, Scott WM, O'Brien FJ, Schmidt TA. The role of synovial fluid constituents in the lubrication of collagen-glycosaminoglycan scaffolds for cartilage repair. *J Mech Behav Biomed Mater.* 2021;118:104445.
30. Morris SM. Arginine: beyond protein. *Am J Clin Nutr.* 2006;83:S508–12.
31. Li Y, Cai H, Fang W, Meng Q, Li J, Deng M, et al. Fibroblast growth factor 2 involved in the pathogenesis of synovial chondromatosis of temporomandibular joint. *J Oral Pathol Med.* 2014;43:388–94.
32. Deryugina EI, Quigley JP. Matrix metalloproteinases and tumor metastasis. *Cancer Metastasis Rev.* 2006;25:9–34.
33. Visse R, Nagase H. Matrix metalloproteinases and tissue inhibitors of metalloproteinases: structure, function, and biochemistry. *Circ Res.* 2003;92:827–39.
34. Xu M, Guo Y, Wang M, Luo X, Shen X, Li Z, et al. L-arginine homeostasis governs adult neural stem cell activation by modulating energy metabolism in vivo. *EMBO J.* 2023;42:e112647.
35. Barr S, Bellamy N, Buchanan WW, Chalmers A, Ford PM, Kean WF, et al. A comparative study of signal versus aggregate methods of outcome measurement based on the WOMAC osteoarthritis index. Western Ontario and McMaster universities osteoarthritis index. *J Rheumatol.* 1994;21:2106–12.
36. Bellamy N, Buchanan WW, Goldsmith CH, Campbell J, Stitt LW. Validation study of WOMAC: a health status instrument for measuring clinically important patient relevant outcomes to antirheumatic drug therapy in patients with osteoarthritis of the hip or knee. *J Rheumatol.* 1988;15:1833–40.
37. Bijlsma JWW, Berenbaum F, Lefeber FPJG. Osteoarthritis: an update with relevance for clinical practice. *Lancet.* 2011;377:2115–26.
38. Shu CC, Jackson MT, Smith MM, Smith SM, Penm S, Lord MS, et al. Ablation of Perlecan domain 1 Heparan sulfate reduces progressive cartilage degradation, synovitis, and osteophyte size in a preclinical model of posttraumatic osteoarthritis. *Arthritis Rheumatol.* 2016;68:868–79.
39. Xu J, Wu M, Yang J, Zhao D, He D, Liu Y et al. Multimodal smart systems reprogramme macrophages and remove urate to treat gouty arthritis. *Nat Nanotechnol.* 2024;1–14.
40. Fan S, Zhang C, Sun X, Su C, Xue Y, Song X, et al. Metformin enhances osteogenic differentiation of BMSC by modulating macrophage M2 polarization. *Sci Rep.* 2024;14:20267.

Publisher's note

Springer Nature remains neutral with regard to jurisdictional claims in published maps and institutional affiliations.